



the society for solid-state  
and electrochemical  
science and technology

Journal of The Electrochemical Society

## Oxide Passivation of Photochemically Unpinned GaAs

P. D. Kirchner, A. C. Warren, J. M. Woodall, C. W. Wilmsen, S. L. Wright and J. M. Baker

*J. Electrochem. Soc.* 1988, Volume 135, Issue 7, Pages 1822-1824.  
doi: 10.1149/1.2096139

---

**Email alerting  
service**

Receive free email alerts when new articles cite this article - sign up in the box at the top right corner of the article or [click here](#)

---

---

To subscribe to *Journal of The Electrochemical Society* go to:  
<http://jes.ecsdl.org/subscriptions>

---

between substrate and incident ion. While RIE is capable of producing nearly vertical wall profiles, altering the wall shape necessitates changes in gas chemistry or adjustment of reactor discharge conditions. Our method for gaining an insight on how contouring of etched features might be influenced was to measure angular etching dependency of several films and gases used in device fabrication under RIE conditions. Results show that oxides and nitrides have an angular dependence resembling a cosine function at low  $\text{CHF}_3$  energy but develop a high-angle etch maximum when ion energy is increased. However, the substrates Si or poly-Si, having lower selectivity to  $\text{CF}_x$  species, give curve shapes resembling a sputtering yield. Photoresist also resembles a sputtering yield under fluorocarbon discharge, but  $\text{O}_2$  and  $\text{NF}_3$  ions show chemical etching of photoresist. Inert ions that have typical sputtering curves provide a method for changing the angular etch curve shape when combined with a chemical etchant.

Angular etching correlations produce three distinct etch characteristics: (i) curve shapes that show material removal purely by chemical etching, in which ion sputtering is minimized; (ii) physical removal through knock-on bombardment, in which yields show a maximum rate at more oblique angles of incidence; and (iii) mixed combinations of physical-plus-chemical or chemical-plus-chemical removal. Condition (iii) provides a method whereby angular dependency is purposely changed during the total etch time. Differential etching is accomplished by admixing two gases during the course of an etch by using computer programming of mass flow controllers. An example is given for a computer controlled flow of  $\text{NF}_3$  into primary etchant,  $\text{CHF}_3$ , resulting in predetermined etch-back of photoresist and oxide to produce a tapered sidewall with rounded corners. Differential etching provides an additional technique for influencing shapes of wall profiles.

Knowledge of angular etching correlations from ion interactions on materials provides data necessary for accurate simulation of the etch process. Using angular yield data, a computer algorithm was developed to model time-rate of material loss and graph two-dimensional profiles similar to our experimental results. By applying etching

simulations based on angular yield data, one can delineate formation of oxide sidewall spacers and reconstruct patterning sequences resulting from structuring trilevel resist masks. These simulations also model RIE of contact holes (vias) based on sequential gas mixing because the angular etch interdependency of oxide and resist is known.

It is concluded that where plasma reactors are amenable to measuring angular etch dependence, an extension of modeling as outlined in this report will bridge the gap between device designers and lithography (processing) laboratories to help meet fabrication requirements.

Manuscript submitted Nov. 3, 1986; revised manuscript received March 3, 1988.

Eastman Kodak Company assisted in meeting the publication costs of this article.

#### REFERENCES

1. P. Sigmund, *Phys. Rev.*, **184**, 383 (1969).
2. M. T. Robinson, "Topics in Applied Physics," Vol. 47, R. Behrisch, Editor, p. 74, Springer-Verlag, Berlin (1981).
3. J. W. Coburn and H. F. Winters, *J. Appl. Phys.*, **50**, 3189 (1979).
4. W. Oldham, S. Nandgaonkar, A. Neureuther, and M. O. O'Toole, *IEEE Trans. Electron Devices*, **ED-26**, 717 (1979).
5. S. M. Rossnagel and R. S. Robinson, *J. Vac. Sci. Technol. A*, **1**, 426 (1983).
6. D. P. Kern and C. B. Zarowin, in "Plasma Processing," R. G. Frieser and C. J. Mogab, Editors, p. 86, The Electrochemical Society Softbound Proceedings Series, Pennington, NJ (1981).
7. G. D. Boyd, L. A. Coldren, and F. G. Storz, *Appl. Phys. Lett.*, **36**, 583 (1980).
8. N. Gellrich, H. Beneking, and W. Arden, *J. Vac. Sci. Technol. B*, **3**, 335 (1985).
9. T. P. Chow, in "VLSI Electronics Microstructure Science," Vol. 8, Academic Press, New York (1984).
10. S. H. Dhong and E. J. Petrillo, *This Journal*, **133**, 389 (1986).
11. W. G. Oldham, A. R. Neureuther, C. Sung, J. L. Reynolds, and S. N. Nandgaonkar, *IEEE Trans. Electron Devices*, **ED-27**, 1455 (1980).

## Oxide Passivation of Photochemically Unpinned GaAs

P. D. Kirchner, A. C. Warren, J. M. Woodall,\* C. W. Wilmsen,<sup>1</sup> S. L. Wright, and J. M. Baker

IBM Research Division, T. J. Watson Research Center, Yorktown Heights, New York 10598

#### ABSTRACT

Using Auger electron spectroscopy and x-ray photoelectron spectroscopy we show that the unpinned GaAs is covered by a  $\text{Ga}_2\text{O}_3$  layer with only small amounts of species containing arsenic. This oxide is formed by the consumption of GaAs during the unpinning treatment. We believe that it is this oxide that passivates the surface, allowing it to remain near flatband for several hours in room air. The near absence of arsenic in the oxide, and the eventual repinning of the surface Fermi level supports the effective work function model of Fermi-level pinning.

Offsey *et al.* (1) reported that the surface of n- or p-GaAs could become nearly flatband even in air if the surface was treated with the combination of flowing deionized water and above bandgap laser light. The sharp reduction in surface band bending was detected by a rise in photoluminescence efficiency that was most pronounced at short wavelength excitation (*i.e.*, response to blue laser light) (2). Both n- and p-type GaAs responded to this treatment, indicating that the surface Fermi level was actually unpinned, unlike other treatments where low surface recombination velocities are obtained by repinning the Fermi level near the appropriate bandedge (3). The capacitance-voltage characteristic of an Hg/PMMA/n-GaAs structure showed control of

the surface Fermi level. Repinning of the surface under continuous  $\sim 0.25 \text{ W/cm}^2$  He-Cd laser light occurs on a time scale of hours (1), while others (4) correctly note that the repinning takes longer in the dark. Although flowing water treatment by Massies and Contour (5) showed a clean GaAs surface, the fact that GaAs could remain unpinned in room air for some time suggested that the surface was protected by a passivating layer.

In this paper (6) we describe a modified photowashing treatment. We characterize the surface oxide which appears to protect the unpinned GaAs surface.

#### Experimental

The original photochemical process (1) is labor intensive, results in a small unpinned area that is not visibly identifiable, and requires care in using the  $\sim 100 \text{ W/cm}^2$

\* Electrochemical Society Active Member.

<sup>1</sup> Present address: Department of Electrical Engineering, Colorado State University, Fort Collins, Colorado 80523.

laser. We tried and adopted for most purposes a similar process designed to produce large area unpinned surfaces. The GaAs wafer is mounted on a photoresist spinner. Tap fed deionized (DI) H<sub>2</sub>O is sprayed onto the central area of the wafer via a PVC hose and an eyedropper nozzle. (Attempts to add oxygen to the water stream have not produced noticeable changes, perhaps because oxygen is available in the ambient). Light is supplied by a 300W tungsten halogen projector bulb with an integral reflector brought within several inches of the wafer.

GaAs wafers were prepared by solvent rinses followed by soaking in 1:1 H<sub>2</sub>SO<sub>4</sub>-H<sub>2</sub>O and etching for 30s in freshly prepared, hot 12:1:3 H<sub>2</sub>SO<sub>4</sub>-H<sub>2</sub>O<sub>2</sub>-H<sub>2</sub>O followed by an H<sub>2</sub>O quench. Under projector bulb illumination, with the wafer spinning at several thousand revolutions per minute, and sprayed with water at ~10 cm<sup>3</sup>/s, a uniform, brilliant blue oxide film is formed in 5-10 min. The color results from interference effects, and oxides thicker than this (~100 nm) are not obtained. "Spotty" oxides often indicate surface contamination. Excessive water flow rates or insufficient illumination result in the lack of observable oxide growth.

To unpin the Fermi level at the GaAs-oxide interface, an activation step is performed following the bulk oxide growth. Illumination is continued while the H<sub>2</sub>O stream is directed off the wafer onto the spinner's rotating aluminum vacuum chuck to keep the GaAs wafer from overheating. Typically several tens of seconds of illumination are sufficient. Alternatively, the laser used in some characterization steps will unpin localized areas. If the wafer is stored in lab air prior to activation, the PL response is reduced from that of freshly prepared samples. Delays of an hour produce a significant degradation. However, the wafer can be stored in desiccated air, in liquid nitrogen, or in high vacuum for days with small (yet detectable) degradation. Activation, however, requires illumination in the presence of certain components of laboratory air. To a large extent, the process resembles the original Offsey *et al.* process which used intermittent spraying of water with continuous spinning and localized laser illumination.

A recently reported unpinning technique (7) involves treating GaAs surfaces with an aqueous solution of heavily hydrated sulfides (e.g., Na<sub>2</sub>S · 9H<sub>2</sub>O). We subsequently employed this method successfully and found that it too required activation (simultaneous exposure to light and laboratory air) and that it underwent light-induced decay. A major difference from the photochemical oxide treatment is that the unpinned sulfide-coated surface is substantially more stable in the dark and in the absence of minority carriers. It appears as if the use of intense above-bandgap light or minority carrier devices to characterize unpinning

treatments has in fact been part of the treatments. The similarities in activation and decay indicate that the two treatments may produce the unpinning effect by the same or related means.

The Auger electron spectrum of a ~100 nm oxide grown by the photochemical process is shown in Fig. 1. Arsenic (in all chemical states) is detected at a ~2% level, with contributions from the oxide, the GaAs substrate, and the ambient of the epitaxy system in which the spectrum was taken. This is in marked contrast to other methods of oxidizing GaAs, such as AGW anodization (8) where the resulting oxide's Ga to As ratio is typically not far from unity.

The x-ray photoelectron spectrum of a much thinner oxide produced by brief treatment is shown in Fig. 2. A very brief photochemical treatment preceded a ~15 min air exposure while the sample was transported to the analysis chamber and loaded through its airlock. In this spectrometer the x-rays were not monochromatized, and as a result elemental and gallium-bonded As are not resolved. However, the core level shifts for oxides of arsenic are substantial enough to allow their differentiation from elemental As and GaAs. Results from curve fitting of the spectrum indicates that the oxide is ~1.2 nm thick and is composed of 90% Ga<sub>2</sub>O<sub>3</sub> and 10% As<sub>2</sub>O<sub>3</sub>. By using different incident angles, the oxides of arsenic are found to be evenly distributed through the thin oxide. Air exposure of the thin oxide may be responsible for the relatively large amounts of As-containing oxides present in the film.

Thus, the following picture of the oxide growth process emerges (6, 9, 10). GaAs is oxidized through the availability of minority carriers and water. The oxides of arsenic are preferentially washed away by the water flow because their solubility in near-neutral water is far greater than that of the oxides of gallium (10). Oxygenation of the water, through the air ambient or through electrolysis, increases the solubility of any unoxidized arsenic. Using the spinner with water but not light removes even thick oxides containing Ga oxides, producing a clean surface (5). This growth mechanism suggests that the oxide should be porous. This is substantiated by the rapid response of the GaAs PL to changes in the gaseous ambient. The photochemical treatment may unavoidably leave trace quantities of species containing arsenic in the film. Only very small quantities are required to produce repinning through reactions that create elemental arsenic at the GaAs-oxide interface (11), such as 2GaAs + As<sub>2</sub>O<sub>3</sub> → Ga<sub>2</sub>O<sub>3</sub> + 4As. This may explain why the GaAs-oxide interface eventually repins in the dark, even in inert ambients (He, N<sub>2</sub>, vacuum).

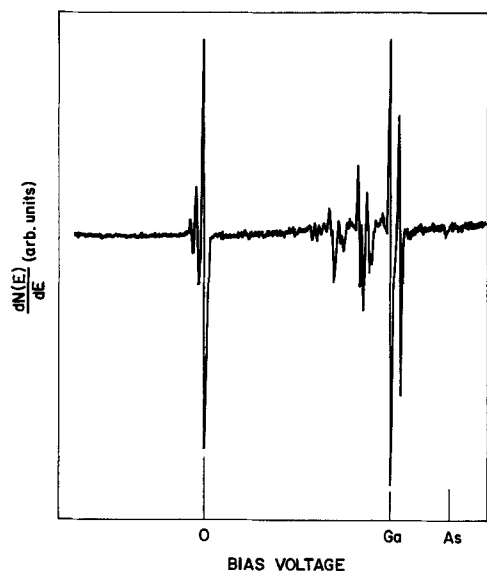


Fig. 1. Auger derivative spectrum of a ~100 nm thick oxide grown by the photochemical process. The primary constituents are gallium and oxygen. Carbon is not detected. Arsenic is present at the ~2% level.

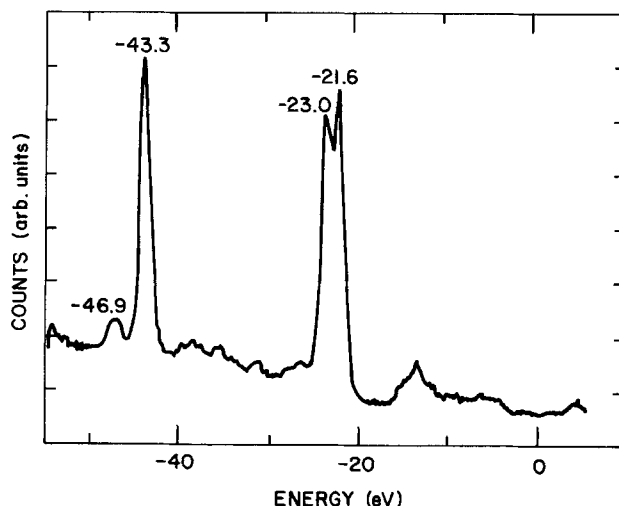


Fig. 2. X-ray photoelectron spectrum of a 1.2 nm thick oxide resulting from brief photochemical treatment. The peak at -21.6 eV is Ga from GaAs. The peak at -23 eV is Ga from Ga<sub>2</sub>O<sub>3</sub>. The peak at -43.3 eV is As from both GaAs and any elemental As. The peak at -46.9 eV is oxidized As. The oxide composition is 90% Ga<sub>2</sub>O<sub>3</sub> and 10% arsenic oxides.

A dense Ga<sub>2</sub>O<sub>3</sub> film could have desirable insulating properties. Experimentally, we have been unable to produce good insulating films with our photochemical technique. Perhaps due to the oxide's alleged porosity, capacitance measurements do not reflect classical metal-insulator-semiconductor behavior. Anodic oxides of GaAs are typically satisfactory insulators. We have formed anodic oxides by the AGW process (8) and attempted to unpin the Fermi level at the anodic oxide-GaAs interface using our photochemical process. But in order to unpin the interface Fermi level, we find that we must remove all the anodic oxide (for instance by using a higher water flow rate and little or no illumination) whereupon the photochemical process will work but a poor insulator is obtained. If we start with our photochemical oxide on GaAs, anodizing it results in rapid repinning.

### Conclusions

The growth of Ga<sub>2</sub>O<sub>3</sub> films on photochemically unpinned GaAs is documented. The Offsey *et al.* technique is modified to produce large-area treated wafers. Attempts to create good insulating films with unpinned GaAs interfaces have been unsuccessful. The recently reported hydrated sodium sulfide treatment (7), in certain aspects of its unpinning and repinning behavior, resembles the photochemical oxides.

### Acknowledgments

The authors thank J. L. Freeouf and E. Yablonoich for valuable discussions.

Manuscript submitted Sept. 3, 1987; revised manuscript received Dec. 10, 1987.

IBM Thomas J. Watson Research Center assisted in meeting the publication costs of this article.

### REFERENCES

1. S. D. Offsey, J. M. Woodall, A. C. Warren, P. D. Kirchner, T. I. Chappell, and G. D. Pettit, *Appl. Phys. Lett.*, **48**, 475 (1986).
2. J. M. Woodall, G. D. Pettit, T. I. Chappell, and H. J. Hovel, *J. Vac. Sci. Technol.*, **16**, 1389 (1979).
3. W. D. Johnston, Jr., H. J. Leamy, B. A. Parkinson, A. Heller, and B. Miller, *This Journal*, **127**, 90 (1980).
4. S. M. Beck and J. E. Wessel, *Appl. Phys. Lett.*, **50**, 149 (1987).
5. J. Massies and J. P. Contour, *ibid.*, **46**, 1150 (1985).
6. P. D. Kirchner, J. M. Woodall, G. D. Pettit, A. C. Warren, S. L. Wright, J. C. Tsang, J. L. Freeouf, and J. L. Baker, in part Paper J-6, Electronic Materials Conference, Amherst, MA, June 25-27, 1986.
7. E. Yablonoich, C. J. Sandroff, R. Bhat, and T. Gmitter, *Appl. Phys. Lett.*, **51** (6), 439 (1987); C. J. Sandroff, R. N. Nottenburg, J.-C. Bischoff, and R. Bhat, *ibid.*, **51**, 33 (1987).
8. H. Hasegawa and H. L. Hartnagel, *This Journal*, **125**, 713 (1976).
9. N. A. Ives, G. W. Stupian, and M. S. Leung, *Appl. Phys. Lett.*, **50**, 256 (1987).
10. J. Van Muylder and M. Pourbaix, in "Atlas of Electrochemical Equilibria in Aqueous Solutions," pp. 516-523, National Association of Corrosion Engineers, Houston, TX (1974).
11. J. M. Woodall and J. L. Freeouf, *J. Vac. Sci. Technol.*, **21**, (574) (1982).

## <sup>18</sup>O Tracer Study of Si Oxidation in Dry O<sub>2</sub> Using SIMS

Chien-Jih Han<sup>1</sup> and C. Robert Helms

Stanford Electronics Laboratories, Stanford University, Stanford, California 94305

### ABSTRACT

Si oxidized sequentially using <sup>16</sup>O<sub>2</sub> and <sup>18</sup>O<sub>2</sub> isotopic tracers was studied in detail to investigate the oxidation mechanisms for dry O<sub>2</sub> oxidation. Analyses of these samples with SIMS provided detail profiles of the <sup>16</sup>O and <sup>18</sup>O concentration in the oxide. At 1 atm and 1000°C, we found <sup>18</sup>O reacted both at the surface of the oxide as well as at the interface. A subsequent anneal of the <sup>18</sup>O oxides revealed that <sup>18</sup>O in both regions of the SiO<sub>2</sub> was incorporated in the lattice. Both <sup>18</sup>O peaks at the surface and at the interface grew with oxidation time. The same <sup>18</sup>O peaks also increased in growth rate with lower initial <sup>16</sup>O<sub>2</sub> oxidation time. The growth rates for both peaks increased at higher temperatures. Profiles of the <sup>18</sup>O in the oxide revealed a solubility limit for the diffusing oxidant in the oxide at 2 × 10<sup>20</sup> cm<sup>-3</sup>. The same profiles also showed very little oxygen diffusion in the network of the oxide ( $D < 10^{-16}$  cm<sup>2</sup>/s).

Although the investigation of silicon oxidation in "dry" O<sub>2</sub> has proceeded for a number of years, there is still considerable controversy concerning the dominant mechanisms, especially for thin oxides. Even for thicker oxides which exhibit nearly parabolic growth behavior, anomalous deviations from a strictly single activation energy diffusion coefficient have been observed (1-3). A major effect is clearly related to the variation of the oxide structure with growth temperature which leads to nonlinear Arrhenius plots for the parabolic rate constant. For thinner oxides, the situation is even more complex. It appears that a strictly interface reaction limited mechanism originally proposed by Deal and Grove (4) is inadequate in explaining the observed effects (4-14), even though this treatment works well in explaining oxidation in steam.

These factors led us to begin an investigation of silicon oxidation in "dry" oxygen (15, 16) using <sup>16</sup>O<sub>2</sub>/<sup>18</sup>O<sub>2</sub> tracer methods. In these studies, oxides were grown initially in <sup>16</sup>O<sub>2</sub> and then in <sup>18</sup>O<sub>2</sub>. The <sup>16</sup>O and <sup>18</sup>O profiles could then be measured and used to determine effects related to the appropriate growth mechanisms. In addition to our work of

this type reported here, Rosencher *et al.* (17), Rochet *et al.* (18), Rouse *et al.* (15), and Costello and Tressler (19) have performed similar experiments. In addition, Mikkelsen (20) used this technique to investigate oxidation effects for steam oxidations, as well as oxygen network diffusion in "dry" oxides (21). Our work uses secondary ion mass spectrometry (SIMS) to obtain better depth resolution and better sensitivity to the oxygen isotopes. The experimental conditions also vary over a wider range than the previous works for a more complete picture of the oxidation process.

To see what we might expect from such experiments, we show an <sup>18</sup>O profile calculated from the Deal-Grove model in Fig. 1. Conditions comparable to our experimental results were chosen with 60 min of <sup>16</sup>O<sub>2</sub> oxidation at 1000°C followed by 30 min of <sup>18</sup>O<sub>2</sub> oxidation at 1000°C. The <sup>18</sup>O profile for such conditions is shown in Fig. 1a, where the value for the oxygen solubility at the surface has been set to 5 × 10<sup>16</sup> cm<sup>-3</sup>. In this profile, the oxide layer at the interface is Si<sup>18</sup>O<sub>2</sub> with the <sup>18</sup>O bonded to the silicon; the <sup>18</sup>O profile in the bulk corresponds to the diffusion profile of unbonded interstitial <sup>18</sup>O<sub>2</sub>. If an inert anneal is performed after the oxidation, the profile of Fig. 1b would be expected, since the

<sup>1</sup> Present address: Honeywell, Incorporated, Bloomington, MN 55420.